Journal of Power Sources 226 (2013) 61–64

Contents lists available at SciVerse ScienceDirect

Journal of Power Sources

journal homepage: www.elsevier.com/locate/jpowsour

Short communication

All-solid-state lithium battery with $LiBH_4$ solid electrolyte

Kuniaki Takahashi [a], Kazuto Hattori [a], Toshihiro Yamazaki [a], Kazunori Takada [b], Motoaki Matsuo [c], Shinichi Orimo [c], Hideki Maekawa [a], Hitoshi Takamura [a,*]

[a] Department of Materials Science, Graduate School of Engineering, Tohoku University, 6-6-11-301-2 Aramaki, Sendai 980-8579, Japan
[b] National Institute for Materials Science, 1-1 Namiki, Tsukuba 305-0044, Japan
[c] Institute for Materials Research, Tohoku University, 2-1-1 Katahira, Sendai 980-8577, Japan

HIGHLIGHTS

- An all-solid-state battery using $LiBH_4$ as a solid electrolyte is prepared.
- $LiBH_4$ has good compatibility with a lithium anode.
- It presents a large resistance at the interface with a $LiCoO_2$ cathode.
- Use of a Li_3PO_4 intermediate layer decreases the interfacial resistance.

GRAPHICAL ABSTRACT

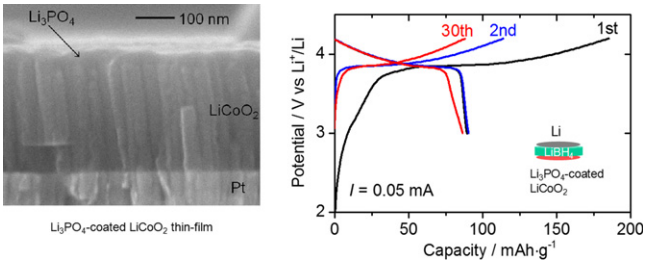

ARTICLE INFO

Article history:
Received 12 September 2012
Received in revised form
19 October 2012
Accepted 25 October 2012
Available online 3 November 2012

Keywords:
Lithium borohydride
Solid electrolyte
All-solid-state battery
Thin film
Pulsed laser deposition

ABSTRACT

Electrochemical properties of all-solid-state lithium batteries using lithium borohydride ($LiBH_4$) as a solid electrolyte are presented for the first time. Despite its high conductivity and good compatibility with a lithium electrode, $LiBH_4$ has not been considered suitable for practical applications partly due to its high reducing capability when used with metal oxides. In our investigation, it was confirmed that contact between this hydride solid lithium ion conductor and $LiCoO_2$ results in a large interfacial resistance, and therefore significant capacity loss. In an attempt to minimize this effect, an intermediate Li_3PO_4 layer was employed. Our results indicate a significant improvement in both the rate and the cycle performance of $LiBH_4$ solid electrolyte batteries, suggesting that $LiBH_4$ can be used in practical applications as an electrolyte in all-solid-state lithium batteries.

1. Introduction

Secondary batteries are essential components of laptops, electric vehicles, cellular phones and other electric devices. Among the various kinds of rechargeable batteries, the lithium battery has the highest energy density; however, since it involves the use of a flammable organic liquid electrolyte, it has been deemed too hazardous for practical applications, when battery size is increased. The use of an inorganic solid electrolyte instead of an organic liquid electrolyte in the battery has been suggested as a way of circumventing this hazard. Various kinds of solid electrolytes have been investigated to date, including oxides and sulfides. Among them, perovskite (ABO_3)-type lithium lanthanum titanate (LLT) [1,2], NASICON with $NaA_2(PO_4)_3$ structure [3,4], LISICON and Thio-LISICON with a γ-Li_3PO_4 framework [5] and garnet-type materials with a nominal $Li_5La_3M_2O_{12}$ composition [6] are well known to exhibit high Li-ion conductivity. Kanno et al. recently reported high conductivity, in the range of 10^{-2} S cm^{-1}, in a novel material, $Li_{10}GeP_2S_{12}$ [7] at ambient temperature, which is comparable to that of conventional organic liquid electrolytes. In addition, amorphous-based conductors such as sulphide-based glass

* Corresponding author. Tel./fax: +81 22 795 3938.
E-mail address: takamura@material.tohoku.ac.jp (H. Takamura).

0378-7753/$ – see front matter © 2012 Elsevier B.V. All rights reserved.
http://dx.doi.org/10.1016/j.jpowsour.2012.10.079

electrolytes and LiPON [8–10], have been the focus of much attention due to their potential for use in all-solid-state lithium batteries. In our study, our focus was on a new class of lithium conductors, lithium borohydride ($LiBH_4$) which shows the structural transition from orthorhombic (LT phase) to hexagonal (HT phase) at about 113 °C [11]. With structural transition, the lithium ion conductivity rises dramatically to the order of 10^{-3} S cm^{-1}. It has been found that the structural transition temperature can be lowered by the addition of a series of lithium halides (LiI, LiBr and LiCl) [12,13]. From an application point of view, while this material shows excellent chemical stability with a Li-metal negative electrode, it comes with the risk of decomposing by reacting with oxidative cathode materials such as $LiCoO_2$. In this investigation, all-solid-state batteries with HT phase $LiBH_4$ solid electrolyte were constructed and their cell performance was determined. Among these batteries was one with an intermediate layer between $LiCoO_2$ cathode and $LiBH_4$ electrolyte.

2. Experimental

2.1. Fabrication process of an all-solid-state battery

A hand-milled mixture of $LiCoO_2$ powder (D10, Toda Kogyo) and $LiBH_4$ powder (Aldrich, >90% purity) in a weight ratio of 10:1 was used as the cathode in a bulk-type cell. For the anode, Li foil (Honjo Metal, >99% purity) was used. An all-solid-state cell was fabricated using a commercial cell assembly according to the following process. The cathode powder and $LiBH_4$ powder were pressed together into a two-layer pellet (φ = 10 mm, t = 1 mm) under a pressure of 3 ton cm^{-2}. Then, Li foil (φ = 9 mm) was placed on the $LiBH_4$ side as the anode. This process was carried out under an Ar atmosphere. The cell was sealed and heated at 120 °C where $LiBH_4$ shows high conductivity. Galvanostatic charge–discharge measurements were carried out at a constant current density of 0.05–0.1 mA (0.065–0.13 mA cm^{-2}) in a potential range between 3.0 and 4.2 V using a potentio-galvano stat (Solartron1470E). Electrochemical impedance spectra were measured by an impedance analyzer (Solartron1260) with an ac voltage of 100 mV in the frequency range of 1 MHz–0.1 Hz.

2.2. Deposition of a Li_3PO_4-coated thin-film cathode

In order to investigate the effects of an intermediate layer on electrochemical performance in all-solid-state cells, $Li_3PO_4/LiCoO_2$ thin-films grown by pulsed laser deposition (PLD) were utilized. The amorphous Li_3PO_4 thin-films with lithium ion conductivity of 4.6×10^{-7} S cm^{-1} at room temperature are obtained by PLD [14]. Li_3PO_4 is known for their good contact with the metal oxides including $LiCoO_2$. Si wafers coated with Pt and Ti were used as the substrate. The $LiCoO_2$ target was a mixture of $LiCoO_2$ and Li_2O (Aldrich) with a weight ratio of 100:15 to compensate for lithium loss during deposition [15]. The Li_3PO_4 target consisted of pure Li_3PO_4 (Aldrich). After the target materials were pelletized, cold isostatic pressing (CIP) was carried out at 250 MPa before sintering. The $LiCoO_2$ and Li_3PO_4 pellets were sintered for 12 h at 850 °C and 1100 °C, respectively. The targets and substrate were placed inside the vacuum chamber of the PLD system at a pressure of less than 10^{-5} Pa. The target-to-substrate distance was kept at 45 mm. A KrF excimer laser with a wavelength of 248 nm (COMPex205, COHERENT) was used for deposition. The laser power and repetition rate were controlled at 300 mJ and 10 Hz for $LiCoO_2$ and at 150 mJ and 5 Hz for Li_3PO_4, respectively. Film deposition was carried out at 300 °C and $P(O_2)$ of 10 Pa for $LiCoO_2$, and at room temperature and $P(O_2)$ = 1 Pa for Li_3PO_4. A fabrication process of cells with this thin-film electrode was as described above for bulk-type cells.

2.3. Structural analysis

Analysis of the thin-films by X-ray diffraction (XRD; Advance, Bruker) was performed using Cu-Kα radiation. The surface morphology and thickness of the thin-films was determined by a scanning probe microscope (SPM; JSPM-5200, JEOL) and a scanning electron microscope (SEM; JSM-6500F, JEOL). Raman spectra were recorded using a Raman system (Horiba JobinYvon, HR-800). A 632.8 nm line from a He–Ne laser was used as the light source.

3. Results and discussion

3.1. Electrochemical performance of the cell using a non-coated $LiCoO_2$ cathode

First, the cell comprises of $Li|LiBH_4|$non-coated bulk $LiCoO_2$ is prepared, and its electrochemical properties will be discussed in this section. The Nyquist plots of a cell using non-coated $LiCoO_2$ powder on the charged-state are shown in Fig. 1. The value of "Re Z" at the high frequency limit (on the left) of the semicircle corresponds to the resistance of the electrolyte, estimated at approximately 60 Ω, which is in good agreement with the reported value [11]. The diameter of the semicircle corresponds to the electrode–electrolyte interfacial resistance. The diameter, at 350 Ω after the 1st charging cycle, increases with increasing cycle numbers up to 1150 Ω after the 10th cycle. Although the initial charge capacity of the cell was 157 mAh g^{-1}, comparable to the theoretical capacity of $LiCoO_2$, the capacity decreased to 68 mAh g^{-1} in the subsequent discharge and further decreased to 18 mAh g^{-1} after the 10th cycle. Since $LiBH_4$ has good chemical compatibility with the lithium electrode, this degradation is clearly attributable to the reaction at the cathode side, indicating the need for modifications at the interface of $LiBH_4/LiCoO_2$ to suppress the large electrode resistance and capacity loss.

3.2. Surface modification to the $LiCoO_2$ thin-film

In an attempt to minimize the electrode resistance and reduce capacity loss, a Li_3PO_4-coated $LiCoO_2$ thin-film was adopted as the cathode. As shown in the SEM image in Fig. 2(a), the film formed was dense, without any pinholes or cracks. The average grain size of the $LiCoO_2$ was approximately 100 nm. The roughness of the Li_3PO_4 layer was determined to be 7.26 nm, as shown in Fig. 2(b), while that of the $LiCoO_2$ layer before Li_3PO_4 growth was 1.99 nm. Large precipitates with a diameter of 1–10 μm appear to be Li_3PO_4 islands; while, smaller ones are $LiCoO_2$ agglomerates. Keeping in mind that the intermediate layer should ideally be as thin as possible, after taking the roughness of the layer into account, it was determined that a 25 nm-thick Li_3PO_4 layer was sufficient to

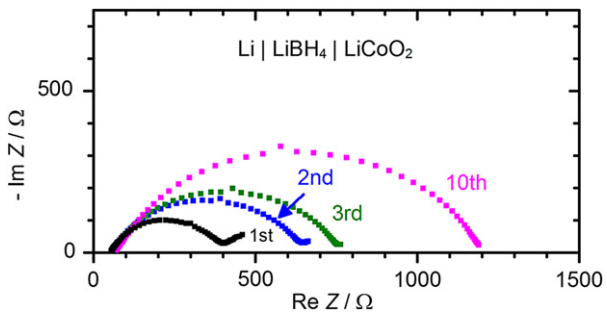

Fig. 1. Nyquist plots of a bulk-type cell ($Li|LiBH_4|LiCoO_2$) on the charged state after 1st, 2nd, 3rd and 10th cycles.

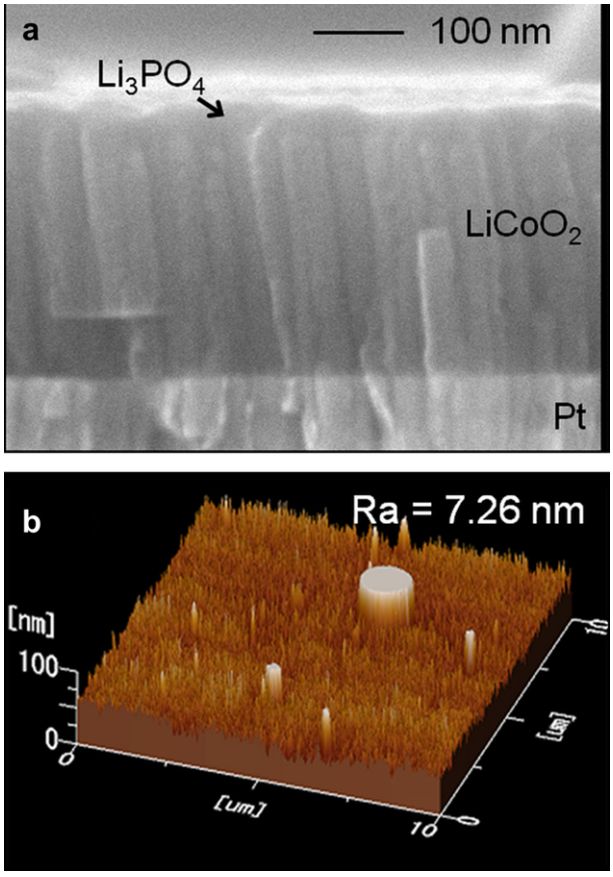

Fig. 2. A cross-sectional SEM image (a) and a surface SPM image (b) of a thin-film $LiCoO_2$ coated with an amorphous Li_3PO_4 layer. The thicknesses of the $LiCoO_2$ and Li_3PO_4 layers were 250 nm and 25 nm, respectively.

fully cover the $LiCoO_2$ surface. The XRD analysis indicated three peaks in the $LiCoO_2$ thin-film, corresponding to the 003, 006 and 009 reflections from rhombohedral $LiCoO_2$, as reported by Xia and Lu [16]. This implies that the $LiCoO_2$ film prepared was *c*-axis oriented. From high-temperature XRD (not shown), it was also confirmed that the crystallization of Li_3PO_4 layer took place at around 750 °C.

3.3. Electrochemical performance of the cell using the Li_3PO_4-coated $LiCoO_2$ cathode

The electrochemical properties of the cells using a $LiBH_4$ electrolyte and $LiCoO_2$ thin-film cathodes with and without a Li_3PO_4 coating are then investigated. The Nyquist plots of a cell with the thin-film cathode are shown in Fig. 3. A cell using a bare $LiCoO_2$ without an intermediate layer (Fig. 3(b)) gave a large semicircle with a diameter of more than 10^4 Ω corresponding to the electrode interface resistance. This interfacial resistance is much larger than that of the bulk-type cell (Fig. 1) presumably due to smaller contact area between $LiBH_4$ and the thin-film $LiCoO_2$, which had a smooth surface. For the $LiCoO_2$ cell with a 25 nm-thick Li_3PO_4 coating, the diameter reduced to around 20 Ω, and almost no change in resistance was observed even after 30 cycles of charge–discharge. The use of the intermediate layer resulted in significant improvements in both the capacity and cycle performance, as shown in Fig. 4. The initial discharge capacity of the cell was estimated at 89 mAh g^{-1} assuming the theoretical density of 5 g cm^{-3} for the $LiCoO_2$ film. It showed high capacity retention

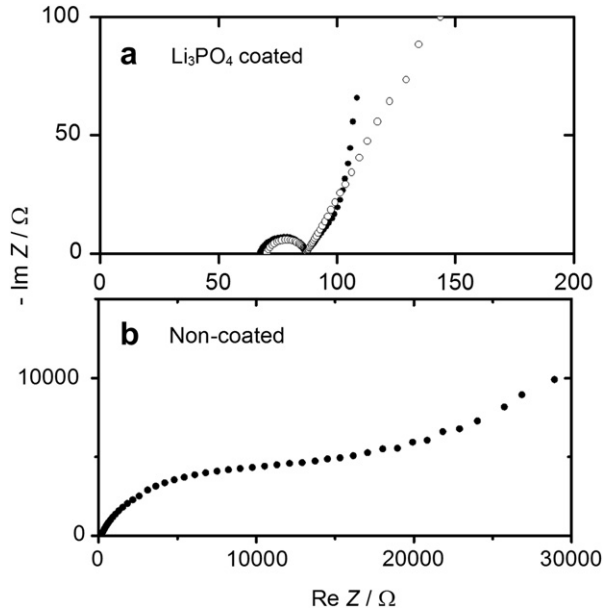

Fig. 3. Nyquist plots of cells with a 25 nm-thick Li_3PO_4 coated $LiCoO_2$ thin-film (a) and with a non-coated $LiCoO_2$ thin-film (b). Filled circles: after 1st charging, White circles: after 30th charging.

upon cycling: the discharge capacity after 30 cycles was more than 97% of the initial discharge capacity, even though the capacity obtained was low with respect to the theoretical capacity for $LiCoO_2$ (140 mAh g^{-1}). This difference in the capacity can be attributed to the low crystallinity of the thin film and the presence of impurities such as lithium oxide and cobalt oxide. The high resistivity in the absence of the intermediate layer can be attributed to the chemical reaction between charged-state $Li_{1-x}CoO_2$ (highly oxidative) and $LiBH_4$, which results in the formation of an insulating layer at the interface. Since $LiBH_4$ is a strong reducing agent, direct contact with transition metal oxides leads to the reduction of the oxide phases.

3.4. Degradation mechanism of the cell using the non-coated $LiCoO_2$ cathode

Further analysis by Raman spectroscopy was carried out in order to clarify the reaction between $LiBH_4$ and $LiCoO_2$. Fig. 5(a) shows

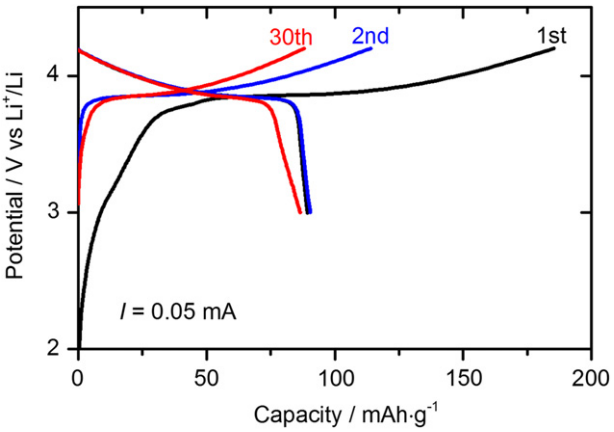

Fig. 4. Charge–discharge curves of a cell with a 25 nm-thick Li_3PO_4 coated $LiCoO_2$ thin-film.

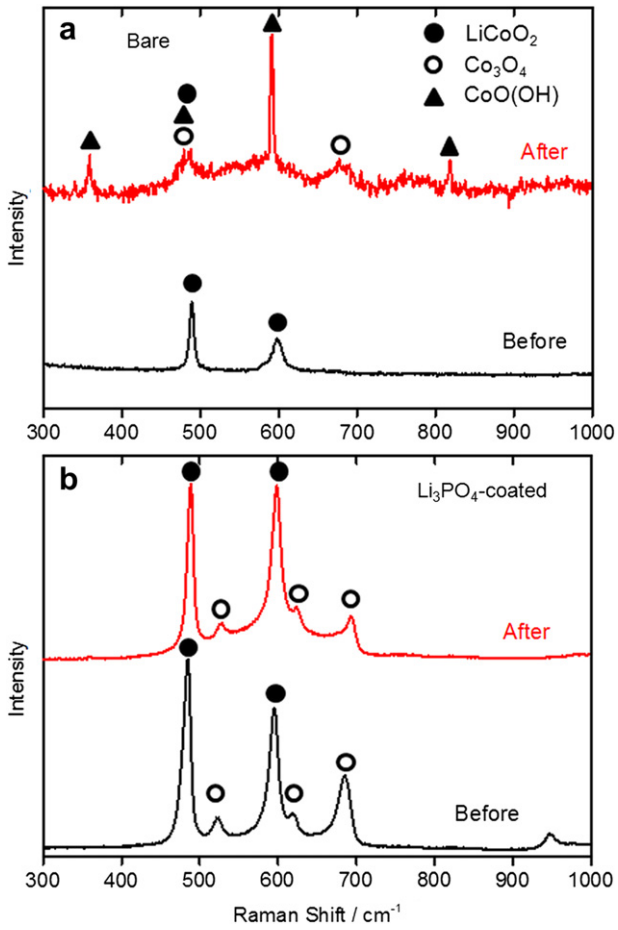

Fig. 5. Raman spectra of a bare $LiCoO_2$ powder (a) and a 25 nm-thick Li_3PO_4-coated $LiCoO_2$ thin-film (b) before and after 30 cycles of charge–discharge.

the Raman spectra of $LiCoO_2$ electrodes ($LiCoO_2$:$LiBH_4$ = 10:1 (wt %)) used for a bulk-type cell before and after 30 cycles of charge–discharge. A $LiCoO_2$ electrode before charge–discharge shows two Raman bands at 482 cm^{-1} and 593 cm^{-1} assignable to E_g and A_{1g} mode of $LiCoO_2$, respectively [17]. This implies that $LiBH_4$ is somewhat stable against discharged-state $LiCoO_2$. After the charge–discharge tests, the $LiCoO_2$ electrode shows four additional peaks at around 360, 590, 680 and 820 cm^{-1} (white circles or filled triangles in Fig. 5) which can be assigned to Co_3O_4 or CoO(OH) [18] as well as $LiCoO_2$ peaks with reduced intensity. This result suggests that $LiBH_4$ reacts easily with charged-state $Li_{1-x}CoO_2$, which leads to the formation of Co_3O_4 and CoO(OH). In contrast, no significant change was observed for a Li_3PO_4-coated $LiCoO_2$ thin-film before and after 30 cycles of charge–discharge as shown in Fig. 5(a), even though Co_3O_4 exists as an impurity in the thin-film regardless of charge–discharge cycles. Taking the fact into account that $LiBO_2$ is generally formed when $LiBH_4$ acts as a reductant, a possible chemical reaction between a fully charged-state $Li_{1-x}CoO_2$ ($x = 0.5$) and $LiBH_4$ was thermodynamically estimated as shown in Eq. (1), even though no resultant compounds except for Co_3O_4 and CoO(OH) were detected in this study.

$$Li_{0.5}CoO_2 + 1/8LiBH_4 \rightarrow 1/4Co_3O_4 + 1/4CoO(OH) + 1/8LiBO_2 + 1/4Li_2O + 1/8H_2 \quad (1)$$

4. Conclusions

The hydride-base lithium ion conductor $LiBH_4$ has the potential to perform as a solid electrolyte in all-solid-state battery applications. A simple cell comprising of $Li|LiBH_4|LiCoO_2$ showed large interfacial resistance due to the reaction of $LiBH_4$ and $LiCoO_2$ at the interface even though the $LiBH_4$ and Li metal have good compatibility. Raman spectroscopy revealed the existence of Co_3O_4 and CoO(OH) in a $LiCoO_2$ electrode after charge–discharge cycles. To overcome the interfacial reaction, a thin Li_3PO_4 intermediate layer between $LiBH_4$ and $LiCoO_2$ was shown to be remarkably effective, reducing the interfacial resistance by three orders of magnitude, and allowing for a discharge capacity of 89 mAh g^{-1} at a constant current density of 0.05 mA cm^{-2}. This cell retains 97% of the initial discharge capacity even after 30 charge–discharge cycles. These results suggest that by utilizing the compatibility between $LiBH_4$ and Li metal, the use of $LiBH_4$ in all-solid-state batteries is possible.

Acknowledgements

This research was financially supported by Advanced Low Carbon Technology Research and Development Program (ALCA) from Japan Science and Technology Agency (JST).

References

[1] Y. Inaguma, C. Liquan, M. Itoh, T. Nakamura, T. Uchida, H. Ikuta, M. Wakihara, Solid State Commun. 86 (1993) 689.
[2] Y. Harada, T. Ishigaki, H. Kawai, J. Kuwano, Solid State Ionics 108 (1998) 407.
[3] V. Thangadurai, A.K. Shukla, J. Gopalakrishnan, J. Mater. Chem. 9 (1999) 739.
[4] M. Sato, T. Suzuki, K. Yoshida, K. Uematsu, K. Toda, Z. Ye, J. Alloy. Compd. 250 (1997) 510.
[5] R. Kanno, M. Murayama, J. Electrochem. Soc. 148 (2001) A742.
[6] V. Thangadurai, H. Kaack, W. Weppner, J. Am. Ceram. Soc. 86 (2003) 437.
[7] N. Kamaya, K. Homma, Y. Yamakawa, M. Hirayama, R. Kanno, M. Yonemura, T. Kamiyama, Y. Kato, S. Hama, K. Kawamoto, A. Mitsui, Nat. Mater. 10 (2011) 682.
[8] Y. Seino, K. Takada, B. Kim, L. Zhang, N. Ohta, H. Wada, M. Osada, T. Sasaki, Solid State Ionics 176 (2005) 2389.
[9] M. Nagao, A. Hayashi, M. Tatsumisago, Electrochim. Acta 56 (2011) 6055.
[10] J.B. Bates, N.J. Dudney, G.R. Gruzalski, R.A. Zuhr, A. Choudhury, C.F. Luck, J.D. Robertson, Solid State Ionics 53–56 (1992) 647.
[11] M. Matsuo, Y. Nakamori, S. Orimo, H. Maekawa, H. Takamura, Appl. Phys. Lett. 91 (2007) 224103.
[12] R. Miyazaki, T. Karahashi, N. Kumatani, Y. Noda, M. Ando, H. Takamura, M. Matsuo, S. Orimo, H. Maekawa, Solid State Ionics 192 (2011) 143.
[13] H. Maekawa, M. Matsuo, H. Takamura, M. Ando, Y. Noda, T. Karahashi, S. Orimo, J. Am. Chem. Soc. 131 (2009) 894.
[14] N. Kuwata, N. Iwagami, J. Kawamura, Solid State Ionics 180 (2009) 644.
[15] C. Julien, M.A. Camacho-Lopez, L. Escobar-Alarcon, E. Haro-Poniatowski, Mater. Chem. Phys. 68 (2001) 210.
[16] H. Xia, L. Lu, Electrochim. Acta 52 (2007) 7014.
[17] M. Inaba, Y. Iriyama, Z. Ogumi, Y. Todzuka, A. Tasaka, J. Raman Spectrosc. 28 (1997) 613.
[18] C. Tang, C. Wang, S. Chien, Thermochim. Acta 473 (2008) 68.